



Forschungszentrum Karlsruhe
in der Helmholtz-Gemeinschaft

Wissenschaftliche Berichte
FZKA 7113

**Actinide Migration
Experiment in the
ÄSPÖ HRL in Sweden:
Results for Uranium and
Technetium with Core #7
(Part IV)**

**B. Kienzler, P. Vejmelka, J. Römer,
D. Schild, Chr. Marquardt, Th. Schäfer,
E. Soballa, C. Walschburger**

Institut für Nukleare Entsorgung

Mai 2005

Forschungszentrum Karlsruhe

in der Helmholtz-Gemeinschaft

Wissenschaftliche Berichte

FZKA 7113

Actinide Migration Experiment in the
ÄSPÖ HRL in Sweden: Results for Uranium and
Technetium with Core #7 (Part IV)

B. Kienzler, P. Vejmelka, J. Römer, D. Schild, Chr. Marquardt,
Th. Schäfer, E. Soballa, C. Walschburger

Institut für Nukleare Entsorgung

Forschungszentrum Karlsruhe GmbH, Karlsruhe

2005

Impressum der Print-Ausgabe:

**Als Manuskript gedruckt
Für diesen Bericht behalten wir uns alle Rechte vor**

**Forschungszentrum Karlsruhe GmbH
Postfach 3640, 76021 Karlsruhe**

**Mitglied der Hermann von Helmholtz-Gemeinschaft
Deutscher Forschungszentren (HGF)**

ISSN 0947-8620

urn:nbn:de:0005-071132

**Actiniden-Migrationsexperiment im schwedischen Untertagelabor ÄSPÖ:
Ergebnisse für Uran und Technetium mit Core #7 (Teil IV)**

Im Rahmen einer bilateralen Kooperation wurde eine Reihe von **Actiniden-Migrationsexperimenten** vom INE im schwedischen Untertagelabor Äspö durchgeführt. Nach mehreren Experimenten zur Migration der Actiniden Am, Np und Pu, werden im vorliegenden Bericht die Untersuchungen zur Uran- und Technetium-Migration in einer Kluft im Granit (core #7) vorgestellt. Um möglichst naturnahe die Migration untersuchen zu können, fanden die Experimente in der CHEMLAB 2 Bohrlochsonde unter in-situ-Bedingungen im Bohrloch KJ0044F01 statt. Es wurde der gleiche Versuchsaufbau wie bei den vorherigen Experimenten verwendet. Der Bericht beinhaltet Ergebnisse zur Fließweg-Charakterisierung mittels Durchbruchkurven des inerten HTO-Tracers. Der Durchbruch von ^{233}U zeigt ein komplexes Muster. Zunächst erscheint ein U-Peak, der geringfügig gegenüber HTO verzögert ist. Diesem schließt sich eine breite Uran-Verteilung an. Nach einer Unterbrechung des Experiments folgt wieder ein scharfer Anstieg und Abfall der Urankonzentration. Die breite ^{233}U -Verteilung stimmt gut mit der anhand von Laborversuchen vorhergesagten Migrationsgeschwindigkeit überein. ^{238}U , welches nicht im verwendeten Tracer vorhanden war, zeigt ein vergleichbares Durchbruchmuster. Die ^{238}U -Konzentrationen werden mit einer Oxidation des natürlichen Urans im Gestein interpretiert. Der Durchbruch von ^{99}Tc erfolgt gleichzeitig mit dem von HTO. Der Wiedererhalt von Tc beträgt ca. 1%.

Abstract

Within the scope of a bilateral cooperation a series of **Actinide Migration Experiment** were performed by INE at the Äspö Hard Rock Laboratory in Sweden. After several experiments investigating the migration of the actinides Am, Np and Pu, this report covers investigations on uranium and technetium migration in a single fractured granite sample (core #7). To provide conditions as close as possible to nature, the experiments are performed in the CHEM-LAB 2 probe under in-situ conditions of the drill hole KJ0044F01 at Äspö HRL. The same experimental setup was used as in previous experiments. Investigations of the flow path properties and the breakthrough of inert HTO tracer are reported. Breakthrough of the ^{233}U tracer shows a complex pattern. Initially, a slightly retarded peak in comparison to HTO appears which is followed by a broad U distribution. After an interruption of the experiment, a sharp ^{233}U peak is observed. The migration velocity of the broad ^{233}U distribution agrees well with the predicted U(VI) migration based on retardation coefficients obtained from batch experiments. Natural ^{238}U which was not present in the used tracer shows a similar pattern as the ^{233}U tracer. The concentrations of natural U are interpreted by oxidation of natural uranium in the core. Breakthrough of ^{99}Tc is observed simultaneously with HTO. Observed Tc recovery is in the range of about 1%.

TABLE OF CONTENTS

1	Background and Objectives	1
2	Properties of the fractured drill core # 7	1
2.1	Mechanical properties.....	1
2.2	Characteristics of the rock material	3
2.3	Hydraulic properties of core #7	4
3	Sorption experiments with uranium and technetium	5
3.1	Batch experiments	5
3.2	XPS investigations of Tc sorbed onto unaltered granite	7
4	U and Tc in-situ migration experiment.....	9
4.1	Cocktail.....	9
4.2	Redox potential.....	9
4.3	Performance of the in-situ migration experiment.....	10
4.4	Elution of radionuclide tracers	11
5	Interpretation and discussion of results	14
5.1	HTO migration and matrix diffusion	14
5.2	Retention of ²³³ U	16
5.3	Retention of ⁹⁹ Tc	18
5.4	Behaviour of natural uranium.....	18
5.4.1	Availability of oxygen	19
5.4.2	Absolute concentration of U.....	21
6	Conclusions from migration and retention experiments	23
7	Outlook.....	25
8	References	26
	Appendix A Tables	27

TABLES

Tab. I	Hydraulic properties of core #7	5
Tab. II	Sorption coefficient of actinides and technetium onto Äspö materials after 14 days of immersion	6
Tab. III	Characteristic data for evaluation of matrix diffusion for core #7	16
Tab. IV	Results of peak fitting for ²³³ U elution in the core #7 experiment	16

FIGURES

Fig. 1	3 D (voxel) representation of the fracture in core #7 determined from X-ray tomography data.	2
Fig. 2	Fracture layer description and some selected parameters for Fracture Type 2. (Widestrand et al., 2003)	3
Fig. 3	XRD analysis of fracture surface material prepared adjacent to the part of the core used for the migration experiment.	3
Fig. 4	Breakthrough of HTO for core #7 at flow rates between 0.17 and 0.0037 ml per minute	4
Fig. 5	Optical scan (a), Fe distribution (b), and α -autoradiography (c) of altered material exposed to ^{233}U spiked solution.	6
Fig. 6	Optical scan (a), Fe distribution (b), and α -autoradiography (c) of freshly broken granite exposed to ^{99}Tc spiked solution.	6
Fig. 7	Narrow scans of Tc 3d spectra (raw data) taken at 4 different areas on the hard rock surface where Tc was detected.	8
Fig. 8	Part of an XPS survey spectrum of the granite sample with Tc sorbed.	9
Fig. 9	Pressure log recorded during the core #7 experiment.	10
Fig. 10	Breakthrough of HTO and ^{233}U tracers during the duration of the migration experiment with core #7.	11
Fig. 11	Breakthrough of HTO and ^{233}U tracers as function of elapsed time in the core #7 in-situ experiment.	12
Fig. 12	Breakthrough of HTO and ^{99}Tc tracers as function of elapsed time in the core #7 in-situ experiment.	13
Fig. 13	Recovery of HTO, ^{99}Tc and ^{233}U over duration of core #7 in-situ experiment.	13
Fig. 14	Breakthrough of HTO and natural ^{238}U as function of elapsed time in the core #7 in-situ experiment.	14
Fig. 15	Relative HTO concentration (C/M_0) and theoretical matrix diffusion line ($t^{-3/2}$) versus elapsed time.	15
Fig. 16	Breakthrough of ^{233}U tracer, ^{99}Tc and the inert HTO tracer as function of eluted volume in the core #7 in-situ experiment.	17
Fig. 17	Breakthrough of ^{233}U tracer and the natural ^{238}U as function of elapsed time in the core #7 in-situ experiment.	19
Fig. 18	Speciation of uranium (activity) (solid lines) and iron (dashed lines) in the groundwater KJ0044F01.	20
Fig. 19	Speciation of uranium (activity) in the groundwater KJ0044F01 assuming different redox states.	21
Fig. 20	Elution of natural uranium in three migration experiments.	22

1 Background and Objectives

The Äspö Hard Rock Laboratory (HRL) was established in Sweden in a granite rock formation for in-situ testing of radioactive waste disposal techniques and for investigations concerning migration and retention of radionuclides (Bäckblom, 1991). Groundwater flow through fractures in granite host rocks may cause migration of radionuclides from the repository. Within the scope of a bilateral cooperation between Svensk Kärnbränslehantering AB (SKB) and Forschungszentrum Karlsruhe, Institut für Nukleare Entsorgung (FZK-INE), actinide migration experiments with Pu, Am, and Np have been conducted in laboratory and under in-situ conditions at the Äspö Hard Rock Laboratory since the year 1999 (Kienzler et al., 2002; Kienzler et al., 2003b; Kienzler et al., 2003c; Römer et al., 2002; Vejmelka et al., 2000). The present paper covers migration and retention studies with uranium and technetium.

The objectives of the FZK-INE investigations are focusing on the quantification of the retention of different actinide elements in individual fractures of a granite host rock and the investigation of the sorption mechanisms. Furthermore, the in-situ actinide migration experiments in the Äspö HRL are directed to examine the applicability of laboratory data to natural conditions and to verify the laboratory sorption studies. Investigations have been performed previously with the actinides Am, Np and Pu. Retention experiments of U and Tc have been done with granite and "fracture filling material" in laboratory. Results are presented elsewhere (Kienzler et al., 2003a; Kienzler et al., 2003c). Migration experiments with HTO, U and Tc through an individual fracture in a drill core have been performed in the Äspö HRL since May 2004. To establish realistic conditions - as close to nature as possible - the experiments are performed in the CHEMLAB 2 probe (Jansson and Eriksen, 1998). This probe confines the drill core, the reservoir with the tracers and the required pump, valves, tubing and control systems. The drill hole interferes a groundwater-bearing fracture at a distance of several meters from the HRL tunnel. Details on the solid materials and the groundwater used in the experiments can be found in a previous publication (Kienzler et al., 2003c).

An important aspect is the quantification of sorbed actinides after termination of the migration experiments. These analyses are not presented in this report, because the experiment is still running.

2 Properties of the fractured drill core # 7

2.1 Mechanical properties

From drill hole KOV 01 778.50-779.25, three parts could be used for migration experiments. Parts of the core #5, #6, and #7 were placed into stainless steel cylinders. The design of

these autoclaves is shown in ref. (Kienzler et al., 2003b). The length of core #7 is 150 mm and the diameter 52 mm. The periphery between cores and steel cylinder wall was filled with epoxy resin. Top and bottom ends are closed with acrylic glass covers. Sealing between the top / bottom ends and the stainless steel cylinder was achieved by O-rings. The lids were provided with fittings for feeding and extracting the groundwater. Tightness of the autoclaves was tested in subsequent laboratory experiments, indicating leak tightness up to 60 bar groundwater pressure. The maximum fluid pressure in CHEMLAB 2 is about 27 bar. The fracture of core #7 was open and its visual appearance is similar to the fracture of core #5.

Prior to the experiments, the internal structures of the embedded drill core were investigated by means of nondestructive X-ray tomography. In ref. (Kienzler et al., 2003c), fracture geometry and sizes of the cores #5 and #7 are determined by evaluation of X-ray tomography data. The aperture for the fracture in the core #7 was determined to be in the range of 0.8 mm. For core #7, the maximum areas of the open fracture (100 mm^2) are located at a distance between 40 mm and 70 mm, and at 120 mm. Minima areas of the open fracture occur in the range from 120 mm to 150 mm (below 40 mm^2).

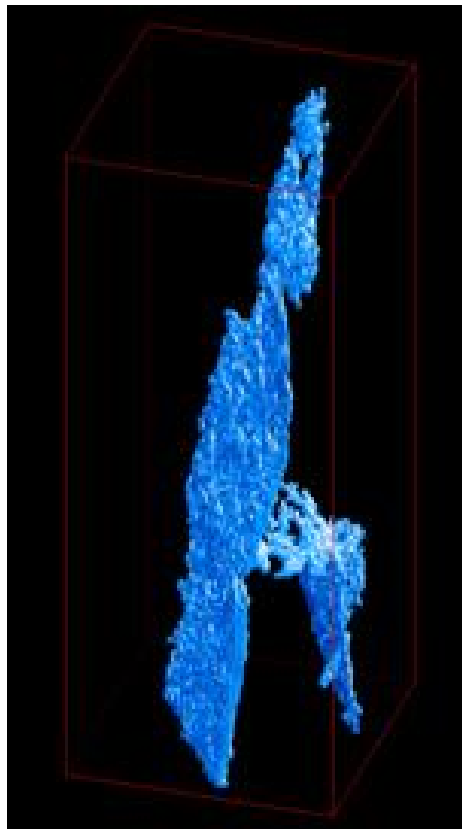


Fig. 1 3 D (voxel) representation of the fracture in core #7 determined from X-ray tomography data.

Fig. 1 shows the complex structure of the fracture. At the bottom of the 3D representation, two fractures are present having certain connectivity. At the top of the picture, the single fracture is twisted.

2.2 Characteristics of the rock material

The solid material is characterised as *Fracture Type 2* using the definition of a recent SKB report (Widestrand et al., 2003) (see Fig. 2).

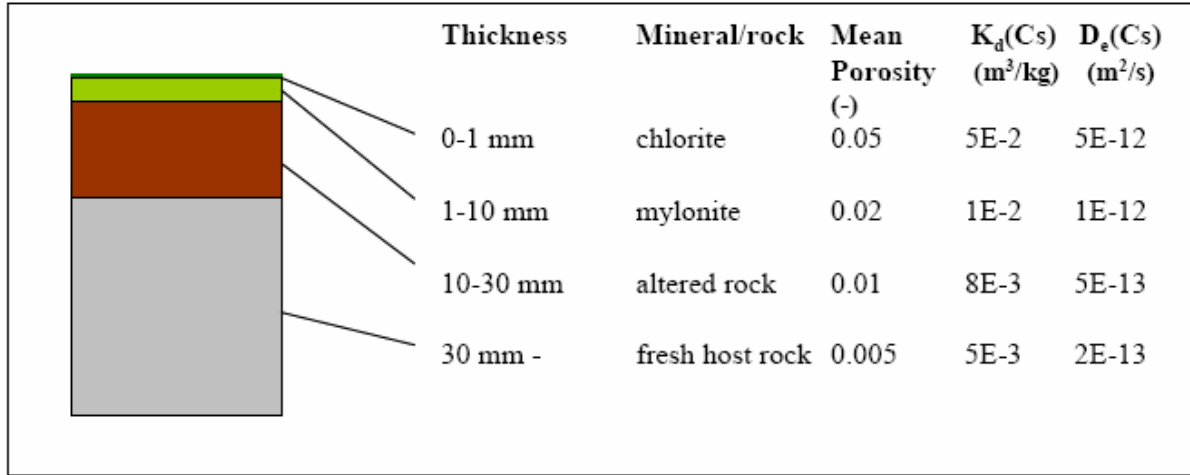


Fig. 2 Fracture layer description and some selected parameters for Fracture Type 2. (Widestrand et al., 2003)

Sorption experiments in laboratory were performed onto samples provided as slices of granite and altered material (fracture surface covering material, untreated, selected planar samples). The solids were characterized and analyzed by scanning electron microscopy (SEM/EDX) and XRD. The granite showed beside the main minerals fine grained Fe-oxides /oxyhydroxides. X-ray diffraction of the altered fracture material showed that chlorite is a main constituent; mica, quartz, and sanidine are also present in this material (Fig. 3).

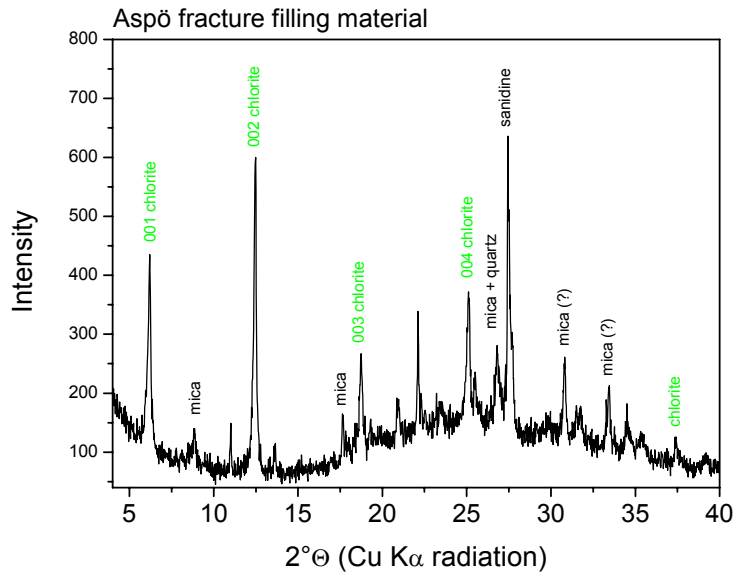


Fig. 3 XRD analysis of fracture surface material prepared adjacent to the part of the core used for the migration experiment.

2.3 Hydraulic properties of core #7

Hydraulic properties, such as effective porosity, dispersion coefficient, and breakthrough time are determined by evaluating measured breakthrough curves of the non sorbing tracer like HTO. HTO breakthrough curves were measured for flow rates between 0.1060 ml/min and 0.0047 ml min⁻¹. Pulse injection of about 50 µl of HTO solution was applied. Breakthrough curves for HTO are shown in Fig. 4. The zeroth, first and second order momentums of the time dependent breakthrough curves are computed corresponding to the mathematical procedure given by Appelo (Appelo and Postma, 1993).

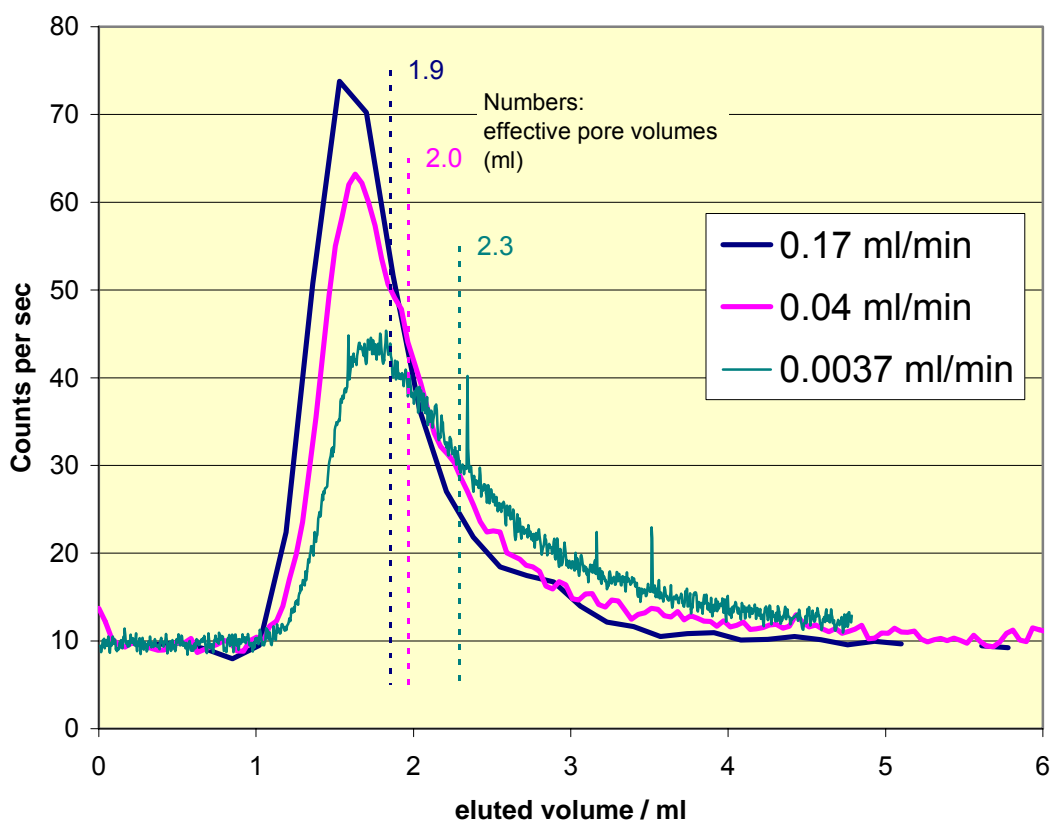


Fig. 4 Breakthrough of HTO for core #7 at flow rates between 0.17 and 0.0037 ml per minute

The hydraulic data are evaluated as described in (Vejmelka et al., 2001). The results are shown in table Tab. I. The effective porosity of the core in volume units is obtained by dividing the Darcy velocity determined from the flow rate by the pore water velocity v_0 . The porosity value given in the table relates the effective porosity to the total volume of the core. Pore volumes of core #7 are ~25% smaller than the values of core #5. It can be seen from the table that in spite of a variation of the flow rate by a factor of almost 50, the dispersion coefficients, the porosities and the Peclet numbers are similar.

Tab. I Hydraulic properties of core #7

Flow rate		0.17 ml/min	0.04 ml/min	0.0037 ml/min
l	m	0.15	0.15	0.15
t₀	s	654±109	2825±495	36700±7300
v₀	m/s	(2.29±0.38)×10 ⁻⁴	(5.31±0.93)×10 ⁻⁵	4.10±0.81)×10 ⁻⁶
σ_t²	-	1.06	1.057	1.07
D	m ² /s	1.8210 ⁻⁵	4.21×10 ⁻⁶	3.30×10 ⁻⁷
α	m	7.94×10 ⁻²	7.93×10 ⁻²	8.08×10 ⁻²
Pore Volume	ml	1.90±0.31	1.97±0.346	2.29±0.45
Porosity	%	0.60	0.62	0.72
Peclet Number	-	1.88	1.89	1.85

3 Sorption experiments with uranium and technetium

3.1 Batch experiments

In order to determine sorption data onto granite and weathered material, sufficiently flat rock samples (size 1.5cm × 1.5cm) were prepared from the fracture adjacent to the part of the drill core used for the migration experiment. The rock samples were pre-equilibrated with Äspö groundwater at anoxic conditions (99% Ar, 1% CO₂) in a glovebox for about 2 weeks. The oxygen concentration were less than 10 ppm. After equilibration, the slices were immersed in ²³³U spiked Äspö groundwater (1×10⁻⁵ mol dm⁻³, 8.4×10⁵ Bq dm⁻³). The exposure periods varied between 1 hour and 14 days. After exposure, the slices were scanned by means of an optical scanner using a resolution of 600×600 pixel per inch. The radioactivity retained on each slice was measured by means of spatially resolved autoradiography (Cyclone Phosphor Scanner, Packard BioScience, Dreieich, Germany) at the same resolution. By calibration of the α-autoradiogram from a rock sample, the absolute activity on the slices was obtained. Composition and area distribution of the mineral phases on the slices was determined by SEM-EDS. To calculate an average surface related retention coefficient, the radioactivity of the solutions was determined by LSC.

Fig. 5 shows the optical scan, the iron distribution determined by element mapping using SEM-EDX and the corresponding α-radiography for a slice consisting of altered material exposed to U. This sample was prepared from a weathered fracture surface. The optical scan shows differently colored phases. Highest Fe concentration is found in brown areas. Light colored parts are identified as feldspar and quartz. The α-autoradiogram correlates well with the Fe distribution, and maxima of retained U coincide with local deposits of Fe oxides.

The sample used for Tc tests was prepared from unaltered granite. In this sample, black areas indicate mainly epidote or chlorite which is in correspondence with the measured Fe distribution. Also for Tc a strong correlation between the Fe and Tc distribution patterns are observed (Fig. 6). Sorption coefficient of actinides and technetium on Äspö materials after 14 days of exposure are shown in Tab. II.

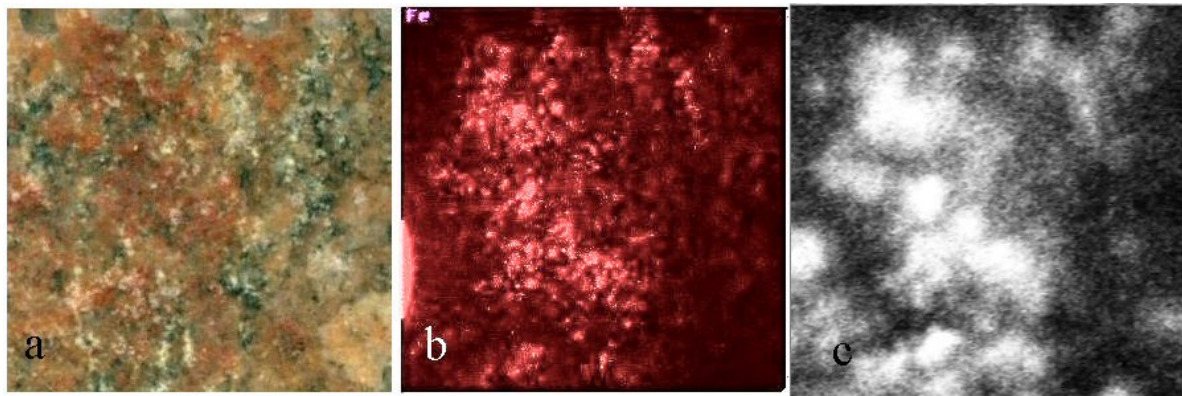


Fig. 5 Optical scan (a), Fe distribution (b), and α -autoradiography (c) of altered material exposed to ^{233}U spiked solution.

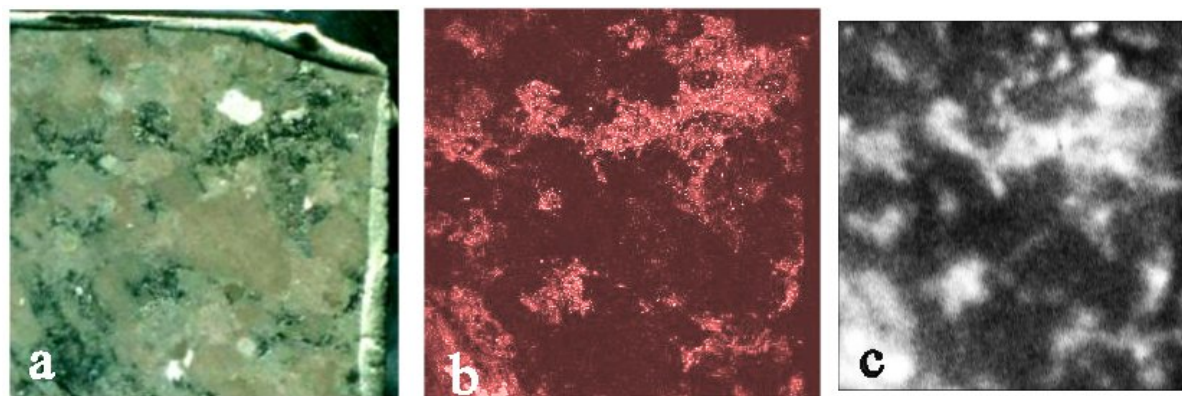


Fig. 6 Optical scan (a), Fe distribution (b), and α -autoradiography (c) of freshly broken granite exposed to ^{99}Tc spiked solution.

Tab. II Sorption coefficient of actinides and technetium onto Äspö materials after 14 days of immersion

	K_s (cm)	freshly broken granite	altered material
^{243}Am		not measured	9.50
^{238}Pu		2.50	1.30
^{237}Np		0.16	0.16
^{233}U		0.026	0.018
^{99}Tc		0.210 ± 0.013	not measured

Tab. II shows significant differences in the retention coefficients between the actinide elements, but less pronounced differences between freshly broken granite and altered materials. The highest sorption within the 14 days period shows Am onto altered material. Mass

for example alkaline or earth-alkaline elements which are expected to shift the binding energy of Tc $3d_{5/2}$ (IV) to lower values. Consideration of the Eh-pH diagram of Tc (Kunze et al., 1996) excludes the presence of Tc(II) which may be indicated by the low binding energy of the Tc $3d_{5/2}$ line.

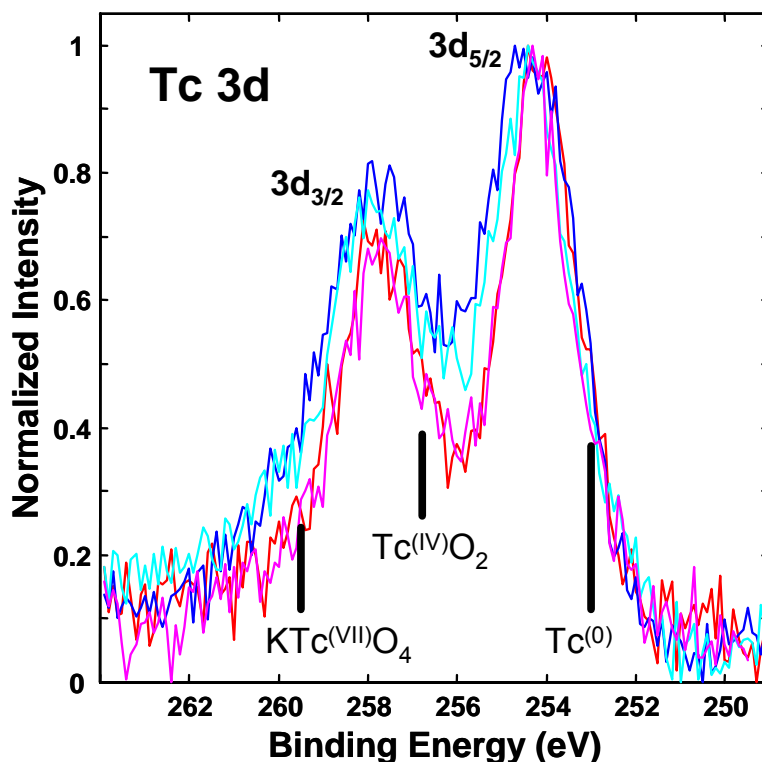


Fig. 7 Narrow scans of Tc 3d spectra (raw data) taken at 4 different areas on the hard rock surface where Tc was detected.

From the table of Appendix A which reflects the element composition according to Fig. 8, an average mineralogical composition of the Tc sorbing phases is calculated to be $M(II)M(III)_2(SiO_4)_2$ which is typical for a feldspar, such as anorthite ($CaAl_2(SiO_4)_2$). This means that Tc retention is not necessarily correlated to high Fe concentrations in the mineral phases. Significant sorption also is observed onto areas free of Fe. However, XPS analyses show a clear shift of Tc binding energy to a reduced redox state. As shown in ref. (Kunze et al., 1996), Tc undergoes reduction in the solution and $TcO(OH)_2(aq)$ may sorb onto the surfaces. A solid surface - as in the case of Np - is not a requirement for the reduction of Tc(VII) to Tc(IV).

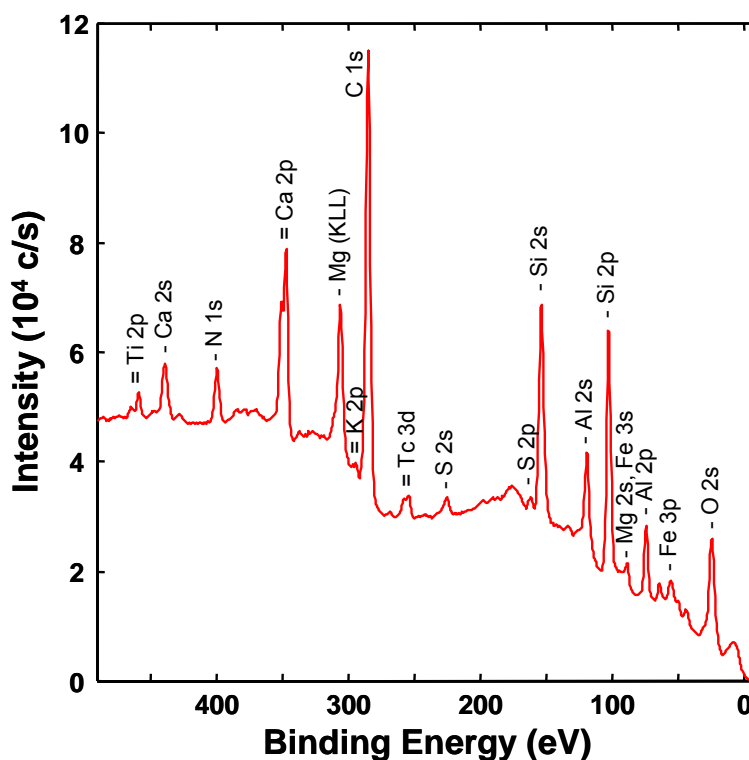


Fig. 8 Part of an XPS survey spectrum of the granite sample with Tc sorbed.

4 U and Tc in-situ migration experiment

4.1 Cocktail

For the in-situ migration experiment with core #7, a cocktail was applied consisting of groundwater SA 2600 spiked by $1.35 \times 10^{-6} \text{ mol l}^{-1}$ ^{233}U , $7.0 \times 10^{-7} \text{ mol l}^{-1}$ ^{99}Tc and 370 Bq ml^{-1} HTO. pH of the cocktail was 7.3, Eh about +70 mV. The concentration of the natural uranium isotope ^{238}U was $2.3 \times 10^{-9} \text{ mol l}^{-1}$, significantly below the ^{233}U tracer concentration.

4.2 Redox potential

Concentrations of main and trace elements in the Chemlab 2 drill hole KJ0044F01 was analyzed by SKB and listed in (Kienzler et al., 2003b). In this publication, Eh between +50 and -200 mV was reported. The setup for redox measurement in a flow through cell was tested in a glove box in laboratory with SA 2600 groundwater in Ar atmosphere. The cell was equipped by an Ionode type SI30 redox electrode. Under these conditions, a potential of -170 mV ($E_h = +74 \text{ mV SHE}$) was measured. This value agrees with previous measurements. In order to verify the redox potential for the migration experiment, the flow through cell was installed in the bypass of Chemlab 2. Potentials were recorded in 10 minutes intervals for more than 16 hours. Mean redox potential of $4.2 \pm 1.1 \text{ mV}$ was obtained which corresponds to $E_h = +248 \pm 1 \text{ mV (SHE)}$. The performance was controlled by a second electrode.

4.3 Performance of the in-situ migration experiment

The core #7 and the cocktail were transferred to Äspö HRL, inserted into Chemlab 2 and a pre-equilibration phase was started in March 2004. After 6 weeks, the flow rate was adjusted to 0.03 to 0.05 ml h⁻¹. In total 10.6 ml of cocktail were injected within a period of 342 hours (14.3 days). Sampling of eluted groundwater was performed by an automatic sampler, changing vials after each 30 hour interval. The vials were sealed to avoid evaporation. Within the first few days, an operating error of the sampler occurred and several sampled volumes have to be united for analysis. The first phase of the experiment lasted from May 13 to July 30, 2004, delivering 62 samples. After the restart of Chemlab 2 in September 3, additional 110 groundwater samples were collected until January 19, 2005. The samples were transported to Forschungszentrum Karlsruhe and analysed with respect to the sampled groundwater volume, the radionuclide concentrations and the groundwater constituents.

During the duration of the experiment, the pressure determined at the packer of Chemlab 2 varied between 50 and 30 bars. At the inlet, pressures were measured between 25 and 21 bars, at the outlet between 25 and 22 bars. The pressure log over the whole duration of the experiment is shown in Fig. 9.

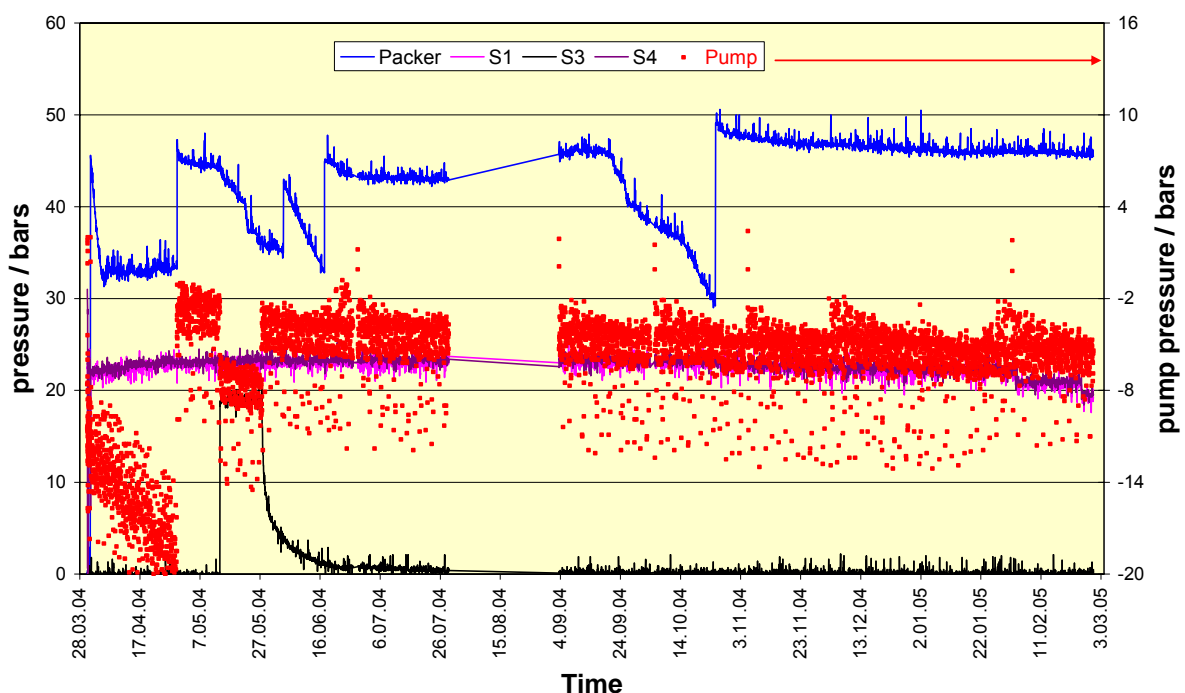


Fig. 9 Pressure log recorded during the core #7 experiment.

Except for the vacation period during August 2004 and some one-day stops due to works on the electricity supply of Äspö HRL, Chemlab 2 worked without any problem. Correct operation of Chemlab 2 is demonstrated by the breakthrough curves of HTO and ²³³U in Fig. 10. The event lines show initially the recovery of the groundwater volume present in the tubing of

Chemlab 2 for ~ 10 days. Then, the event line^a indicates expected arrival of the injected cocktail. The experiment was interrupted from July 30 to September 03, 2004, and for another 2 days in October.

4.4 Elution of radionuclide tracers

The HTO peak is found as expected: During a first phase of cocktail injection, the peak evolved and decreased again, after switching from cocktail to groundwater flow, the HTO concentration dropped until July 30 continuously. Onset of breakthrough of ²³³U is retarded by ~8 days in comparison to the HTO curve. After reaching a minimum, of the ²³³U concentration at June 30, the concentration increased again until interruption of the experiment. After 37 days of interruption, peaks of U and HTO occurred, decreasing to the previous level within ~10 days. End of October 2004, HTO reached detection limit, U remained at a constant concentration. (The scatter of ²³³U concentrations between beginning and end of June 2004 is the result of using both LSC and ICP-MS measurements in the same diagram Fig. 10.)

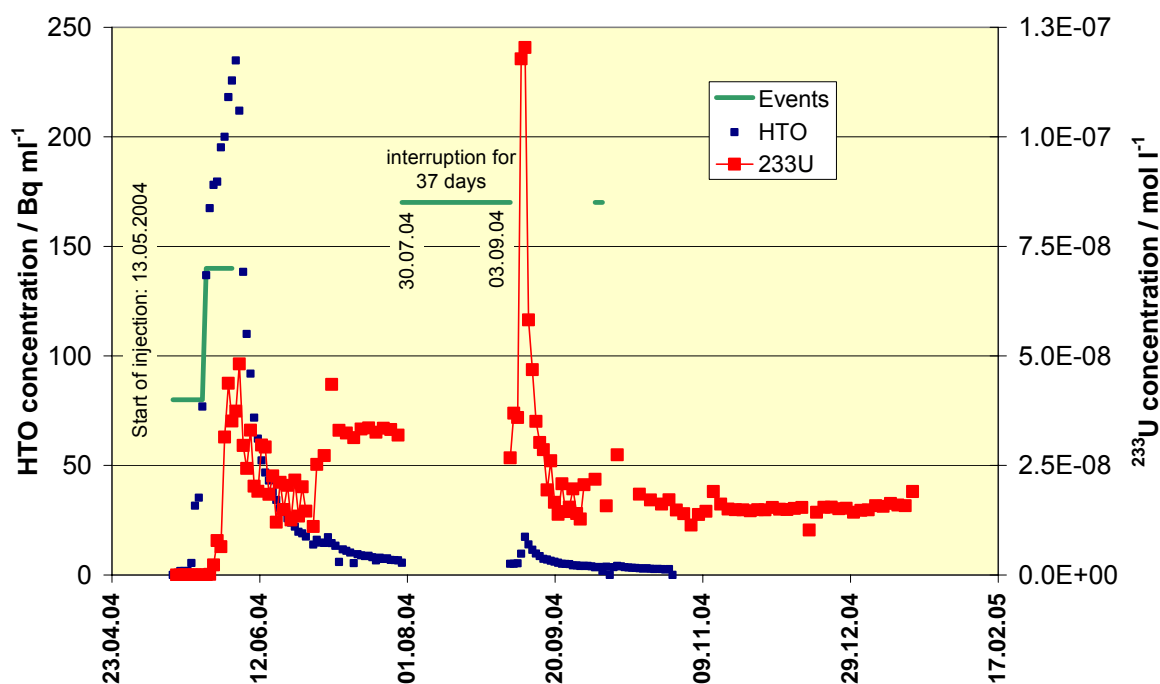


Fig. 10 Breakthrough of HTO and ²³³U tracers during the duration of the migration experiment with core #7.

^a The event line shown in the diagrams indicates specific actions in the Chemlab 2 operation, such as arrival of dead volumes, tracer injection or interruptions of the experiment.

All radionuclides including the natural ^{238}U (see Fig. 14) show an initial peak close to the HTO peak. After the interruption of the experiment in September 2004, a small HTO peak occurs and pronounced peaks for the U tracer and the natural U (see below).

For interpretation of the breakthrough curves, actual time is converted in elapsed time or eluted volume, respectively. In the scale of elapsed time, the breakthrough of HTO and ^{233}U or ^{99}Tc tracers as function of elapsed time in the core #7 in-situ experiment is shown in Fig. 11 and Fig. 12. The error bars indicated in both figures are obtained by error propagation assuming a 10% error in each volume determination and 5% error in the ICP-MS concentration measurements.

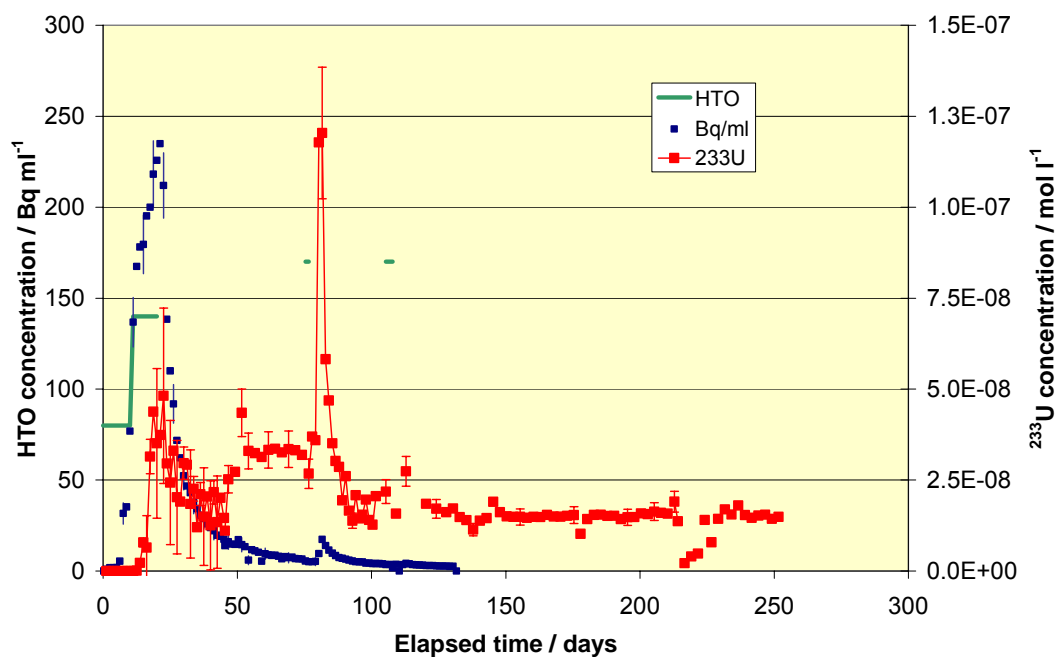


Fig. 11 Breakthrough of HTO and ^{233}U tracers as function of elapsed time in the core #7 in-situ experiment.

^{99}Tc was eluted simultaneously to the inert tracer HTO (Fig. 12). After the peak, the concentration dropped and remained close to the detection limit during the whole experiment. In total, recovery of HTO amounted $> 100\%$, 36 % for ^{233}U (after 254 days) and $\sim 1\%$ ^{99}Tc of the injected quantities. Fig. 13 shows the recovery of HTO, ^{99}Tc and ^{233}U over duration of core #7 in-situ experiment. The amount of uranium estimated from both peaks of the U tracer curve (at the beginning of the experiment and after the interruption see Fig. 11) contribute only by 5% each to the total recovery.

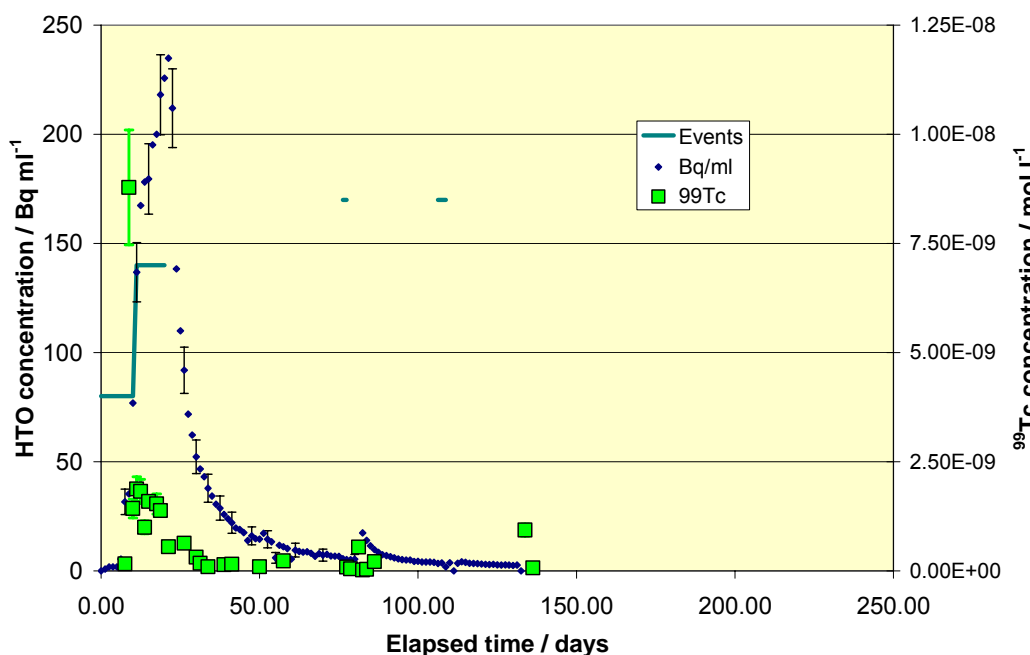


Fig. 12 Breakthrough of HTO and ^{99}Tc tracers as function of elapsed time in the core #7 in-situ experiment.

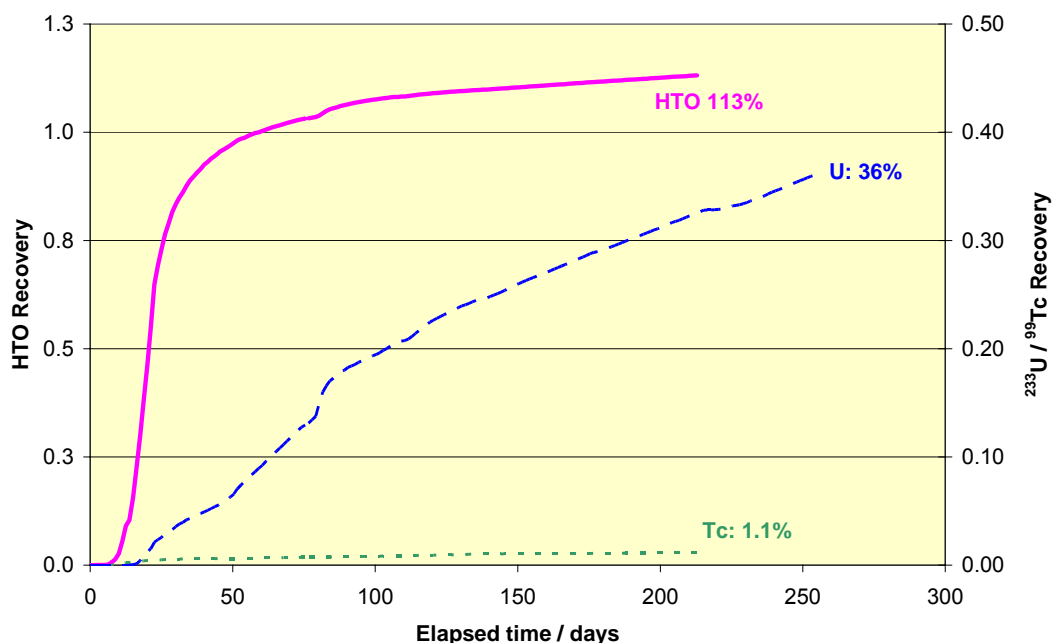


Fig. 13 Recovery of HTO, ^{99}Tc and ^{233}U over duration of core #7 in-situ experiment.

The concentration of natural ^{238}U was measured in addition to the applied tracers (Fig. 14). Onset of breakthrough of natural ^{238}U occurs simultaneously to the breakthrough of HTO. Similarities and differences of ^{238}U migration to the ^{233}U tracer are discussed below (Chapter 5.4 Behaviour of natural uranium).

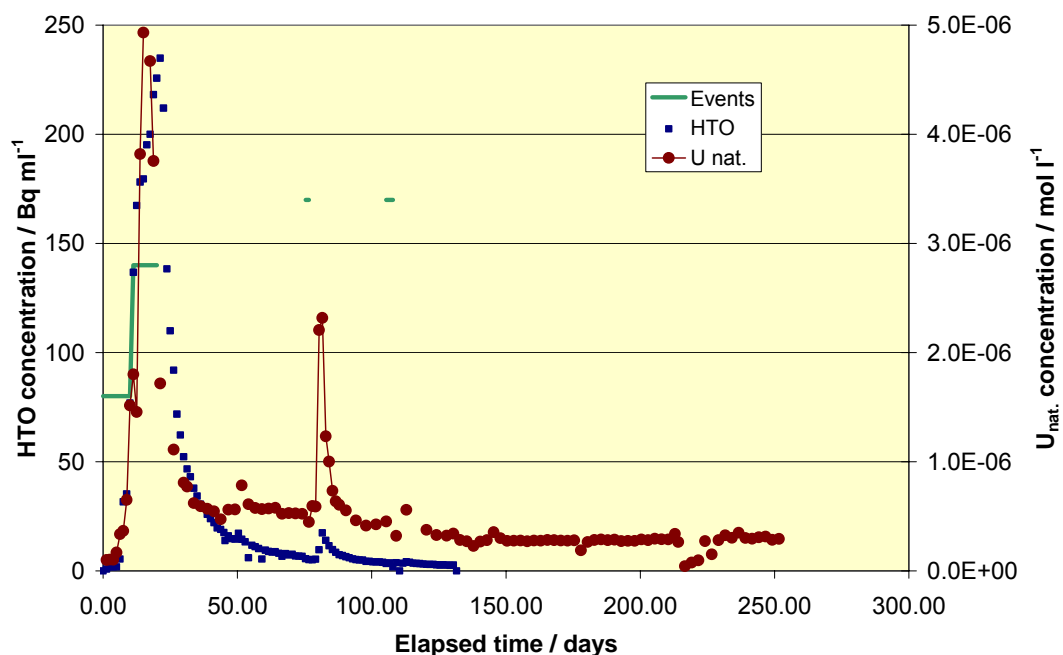


Fig. 14 Breakthrough of HTO and natural ^{238}U as function of elapsed time in the core #7 in-situ experiment.

5 Interpretation and discussion of results

The core #7 experiment confirms one observation which has been found also in the previous experiments: A breakthrough of radionuclide tracers occurred simultaneously with the breakthrough of the inert tracer. In the present experiment, this was observed for Tc and U, former experiments showed this behaviour for Np. Am breakthrough was detected close to the detection limit (core #1 experiments). In the core #7 experiment, the recovery of U is about 33%, whereas the Tc recovery is $\sim 1.1\%$. Recovery of Np in the previous experiments varied between zero and 40%. The reason for the initial “unretarded” breakthrough of these elements is correlated with the retention kinetics described in chapter 3. “Sorption experiments with uranium and technetium”. Elements with fast retention (Am) show a breakthrough only in the case of high flow rates (core #1 experiments) at very low concentrations (detection limit). Elements reacting at slower rates (U, Tc) show an initial breakthrough. The same was observed for Np in previous tests. Breakthrough of Pu was never detected.

5.1 HTO migration and matrix diffusion

Using the inert HTO tracer, the relevance of matrix diffusion was tested. Fig. 15 shows that the measured decrease of the inert tracer concentration is faster than the predicted decrease in the case of matrix diffusion from an infinite volume.

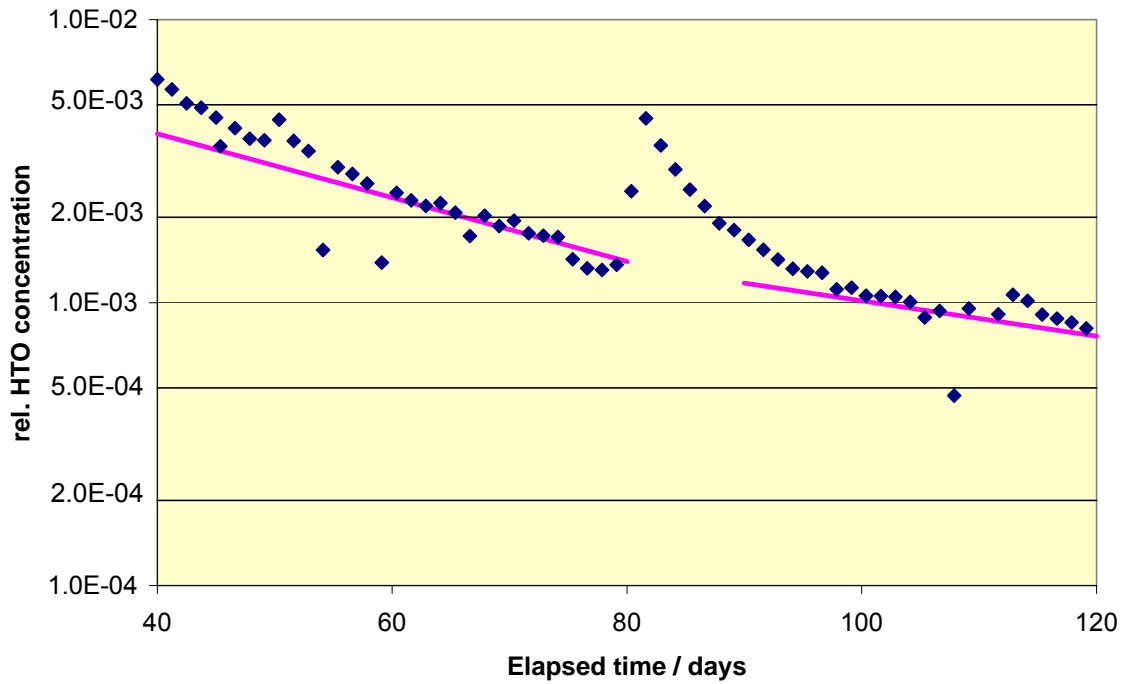


Fig. 15 Relative HTO concentration (C/M_0) and theoretical matrix diffusion line ($t^{-3/2}$) versus elapsed time.

Fig. 15 shows a HTO peak at elapsed times between 80 and 100 days. This peak occurs directly after the interruption of the experiment. Integrating this peak delivers a ~4% contribution of this peak to the totally eluted HTO. Small maxima occur also at 50 and at 113 days. These peaks are correlated to short interruptions of the experiment at June 27 and October 5, 2004 and are too small to be quantified. ^{233}U and ^{99}Tc data do not show any tendency which has to be interpreted by matrix diffusion processes.

For evaluation of the breakthrough curve in terms of matrix diffusion, an analytical solution of diffusion from a well stirred solution of limited volume (see (Crank, 1978), equation 4.37) is applied (eq. 2).

$$\frac{M_t}{M_\infty} = 1 - \sum_{n=1}^{\infty} \frac{2\alpha(1+\alpha)}{1+\alpha+\alpha^2q_n^2} \exp\left(-\frac{Dq_n^2t}{l^2}\right) \quad \text{eq. 2}$$

where α is the ratio of the volume of the solution to the volume of the sheet. q_n are computed by eq. 3. M_t represents the diffused mass at time t .

$$q_n = \left(n + \frac{1}{2}\right)\pi \quad \text{eq. 3}$$

For application of eq. 2, characteristic data are used in the same way as shown by ref. (Widstrand et al., 2003). These data are listed in Tab. III. The gauge aperture a (half-width of the fracture) is 0.4 mm for core #7, l defines the depth of the disturbed/alterd wall of the

fracture; D is the diffusion constant of the altered rock and the relevant period of time t is given by the interruption of the experiment. Porosity corresponds also to the altered rock.

Tab. III Characteristic data for evaluation of matrix diffusion for core #7

Property	Value	Units
a	0.4	mm
l	5 to 10	mm
D	1.00E-12	m ² s ⁻¹
	8.64E-04	cm ² d ⁻¹
t	37	days
$\alpha = a/l$	0.04	
Porosity	0.03	

Using data of Tab. III, it is computed that within 37 days almost 50% the HTO which has been diffused into the matrix is released into the fracture. Computing the average HTO concentration in the matrix shows that before interruption of the experiment the HTO concentration in a 5 mm layer adjacent to the fracture was $\sim 3 \text{ Bq cm}^{-2}$.

5.2 Retention of ²³³U

In the ²³³U concentration curve, several peaks are found (Fig. 16). Five peaks can be fitted by deconvolution of the elution curve in terms of Gaussian functions. The results are given in Tab. IV

Tab. IV Results of peak fitting for ²³³U elution in the core #7 experiment

	Elapsed time days	Width days	Eluted volume ml	Max. concentration mol l ⁻¹
Peak 1	23.1	13.0	21.4	4.0E-08
Peak 2	51.9	3.4	59.1	4.2E-08
Peak 3	68.1	53.6	80.4	3.4E-08
Peak 4	81.2	2.81	96.6	1.2E-07
Peak 5	114.7	6.8	138.7	2.6E-08

The first ²³³U peak occurs close to peak of the inert HTO tracer. According to the momentum method (Vejmelka et al., 2000) the U travel velocity is $6.2 \times 10^{-3} \text{ m s}^{-1}$ (HTO: $7.5 \times 10^{-3} \text{ m s}^{-1}$). Analyzing the broad peak of the ²³³U curve between 50 ml and 120 ml (neglecting the high peak at 94 and 104 ml), a migration velocity of uranium of $2.1 \times 10^{-3} \text{ m s}^{-1}$ is computed.

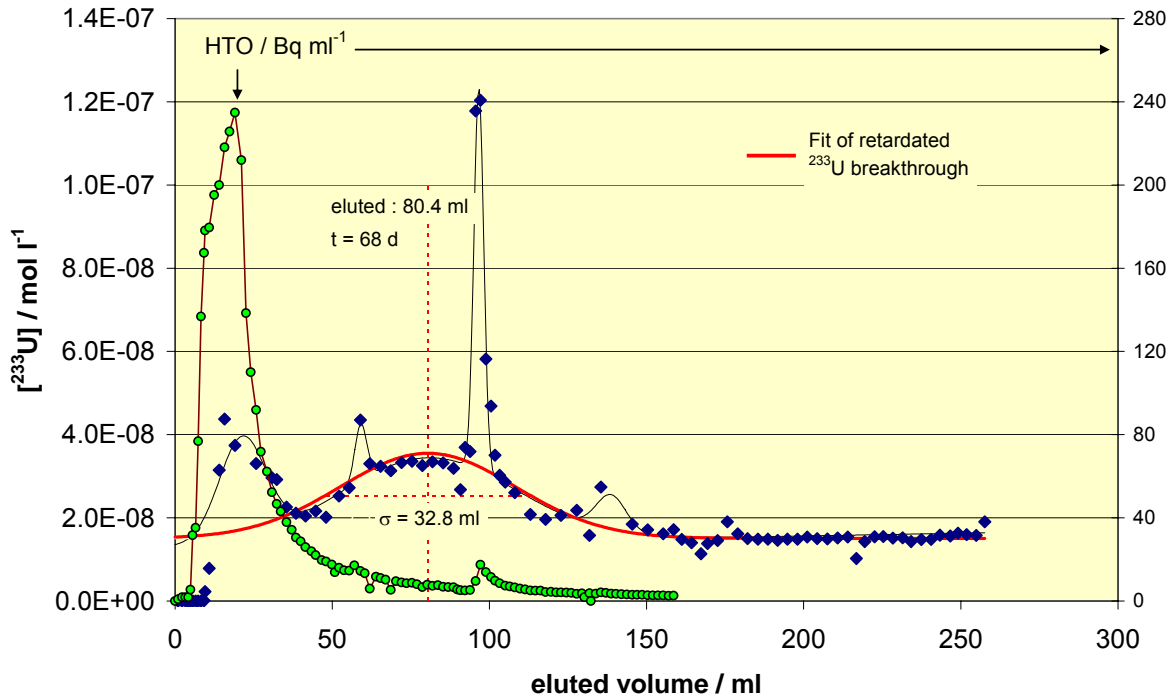


Fig. 16 Breakthrough of ^{233}U tracer, ^{99}Tc and the inert HTO tracer as function of eluted volume in the core #7 in-situ experiment.

From deconvolution of the elution curve, the centre and the width of the retarded U concentration between 50 ml and 120 ml is computed to 80.4 ml (Peak 3 after 68 days) for the centre and a width of the Gaussian of ± 32.8 ml (see Fig. 16 and Tab. IV). The ratio between the centres of the eluted volume curves for U (solid red line) and for HTO results in $R_s = 3.9$ for the retardation coefficient with respect to advective transport processes.

The R_s value of 3.9 is a little bit lower than expected from the batch experiments (see Chapter 3 “Sorption experiments with uranium and technetium”, eq. 1). However, one has to keep in mind that for scaling the batch sorption data to core test, the shape factor of core #5 is applied. The slight difference from 3.9 (core #7 experiment) to 5 (calculated from core #5 and batch data) may be a result of the different fracture properties of core #7 in comparison to core #5 (e.g. pore volume $\sim 25\%$ difference, see chapter 2.3 Hydraulic properties of core #7).

After the restart of Chemlab 2 (eluted volume 91 ml), a sharp ^{233}U peak (4) appears which is recorded at several liquid samples. The maximum concentration is by a factor of ~ 3 above the concentration during the initial peak. After 114.7 days (136.7 ml) a 5th peak is found. Peak 1 is interpreted by a slow kinetics of the retention reactions and peak 3 is explained by reversible sorption with a $R_s = 3.9$. Peak 2, 4 and 5 seem to be correlated to interruptions of the elution (see event line in Fig. 11). If the flow stops for some time, U tracer which has undergone matrix diffusion may come into equilibrium again. This hypothesis is supported by the fact that after the long interruption of the flow the concentrations (peak 4) are significantly higher than after some short events (peak 2 and 5). Also the relatively high constant concentration level after the 5th peak gives rise to the assumption that ^{233}U tracer is released from the rock matrix. A correlation to matrix diffusion as shown in Fig. 15 for HTO is not possible in this simplified manner. Evaluation requires detailed numerical analysis.

5.3 Retention of ^{99}Tc

Fig. 12 reveals the breakthrough of ^{99}Tc . In contrast to uranium, after the initial peak together with HTO, Tc concentration decreases to values close to the detection level of $1 \times 10^{-10} \text{ mol l}^{-1}$. This behaviour is rather similar as found in previous experiments with neptunium. It was shown that Np(V) is reduced to Np(IV) (Kienzler et al., 2003a). As shown in the XPS investigations (see Chapter 3.2 XPS investigations of Tc sorbed onto unaltered granite) Tc in reduced state is retained. Tc retention is not necessarily correlated to high Fe concentrations in the mineral phases. Tc undergoes reduction in the solution which is facilitated by the low redox potential of the groundwater.

5.4 Behaviour of natural uranium

From the U concentrations in the water sampled during the core #7 experiment, it is found that ^{238}U is less retarded than the tracer ^{233}U (by ~8 days in comparison to HTO). The natural uranium concentrations (including the isotopes 238, 235 and 234) show a peak and drop afterwards. The second peak after the interruption of the experiment is also present. Between the two peaks the ^{238}U concentration is more or less constant and tends again to a constant concentration after the decay of the second peak after the 37 days of interruption. In total, $1.7 \times 10^{-7} \text{ mol}$ of ^{238}U is eluted.

The simultaneous breakthrough of the artificial and of the natural uranium raises questions. In the literature (Ilton et al., 2004; Rodrigues et al., 1998), a reduction of U(VI) to U(IV) on relevant granite mineral phases is described. This reduction process is also observed onto pure magnetite. In this study (Aamrani et al., 1999), the interaction between U(VI) and the surface of magnetite is reasonably well described by means of a surface complexation model involving the formation of two different surface complexes. The study of the surface of the solid by means of XPS indicates that the initial attachment of U(VI) to magnetite may be followed by a much slower process of electron transfer which would imply the reduction of U(VI) to U(IV) and the subsequent oxidation of Fe(II) to Fe(III). From the binding energy of the $\text{U}4f_{7/2}$ peak, it is concluded that the reduction of U(VI) does not take place at acidic pH, but in the presence of carbonate.

U concentration in equilibrium with U(IV) minerals, such as $\text{UO}_2(\text{am})$ would result in concentrations of $1.2 \times 10^{-9} \text{ mol l}^{-1}$. Equilibrium with coffinite or uraninite would result in concentrations by several orders of magnitude lower. However, in core #7 experiments, after more than 200 days elapsed time, the eluted ^{238}U concentration is in the range $2\text{-}3 \times 10^{-7} \text{ mol l}^{-1}$ which surmounts the ^{233}U concentration by a factor of ~20. ^{238}U was not added to the injected cocktail. A comparison of the breakthrough curves of both isotopes is shown in Fig. 17. The correspondence of the peaks is obvious, besides the absolute concentrations, the shoulder of the ^{233}U curve between 50 and 100 days indicates a different behaviour of the two isotopes.

Several assumptions are considered to explain the natural U concentrations: The assumptions cover a pH drop, increase of CO₂ partial pressure, and effects due to oxygen contamination either in the Chemlab 2 drill hole KJ0044F01, in the Chemlab 2 probe or in core #7. pH increase is ruled out and is additionally confirmed by the constant concentrations of mineral forming elements. Increase of CO₂ would also affect the pH.

The following hypothesis is formulated for the interpretation of the uranium findings:

- Both uranium isotopes are present in the hexavalent redox state in solution and the solubility is controlled also by hexavalent mineral phases.

To prove this hypothesis, the following conditions have to be kept in mind:

- Groundwater KJ0044F01 has a negligible natural U concentration of 0.16 µg l⁻¹.
- Cocktail (SA 2600) groundwater has a measured natural U concentration of 0.5 µg l⁻¹.
- ²³³U tracer is injected in the redox state U(VI).
- Since drilling, the core was stored for several years in air.

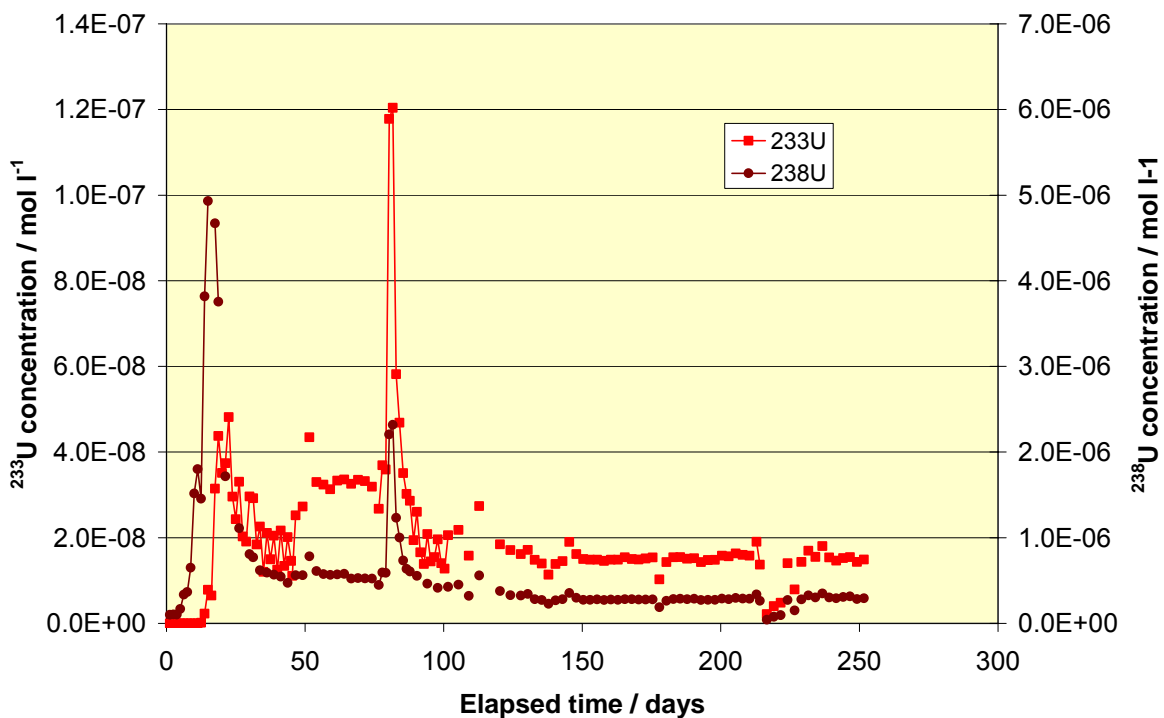


Fig. 17 Breakthrough of ²³³U tracer and the natural ²³⁸U as function of elapsed time in the core #7 in-situ experiment.

5.4.1 Availability of oxygen

Different sources of oxygen may react during the experiment. Since drilling and during storage of the drill core, the rock matrix of core #7 is contacted to oxygen of the air. This contact does not only influence the outer surfaces of the core but also the surfaces of the fracture and the pores which were present originally or which may have been formed as a conse-

quence of stress release during drilling. Uranium minerals may be oxidized in the way that natural U(IV) minerals are converted to U(VI) minerals to some extent. However, it would also be possible that O₂ is sorbed onto the surfaces of the core and starts reacting when groundwater contacts the surfaces during the experiment.

In KJ0044F01 groundwater, the [Mn] = 420 µg l⁻¹ and 570 µg l⁻¹ in the groundwater (SA 2600) used for the cocktail. During the initial peak, the Mn concentration dropped by a factor of ~5 which may indicate the influence of an oxygen contamination in the core #7 or in the cocktail reservoir. After the tracer injection was eluted, the Mn concentration increased again to a constant concentration corresponding to the undisturbed KJ0044F01 water. The Fe concentration scattered between 150 and 300 µg l⁻¹ indicating no specific pattern.

In total, within 254 days of experimental time, 1.7x10⁻⁷ mol of ²³⁸U is eluted. To oxidize this quantity of U(IV), the same equivalent of oxygen is required. For Äspö's fracture minerals, an O₂-uptake rate of 1.3 - 5x10⁻⁵ mol L⁻¹ day⁻¹ was determined^b (Puigdomenech et al., 2001). In this reference, only reactions with iron minerals are discussed. In the same report, O₂-uptake related to surfaces is listed for Canadian granite of about 1.3x10⁻⁵ mol m⁻² day⁻¹. This high rate shows that within a few days the O₂-uptake is sufficient for the U(IV) to U(VI) oxidation. In this paper, interactions of oxygen with U(IV) phases have not been considered.

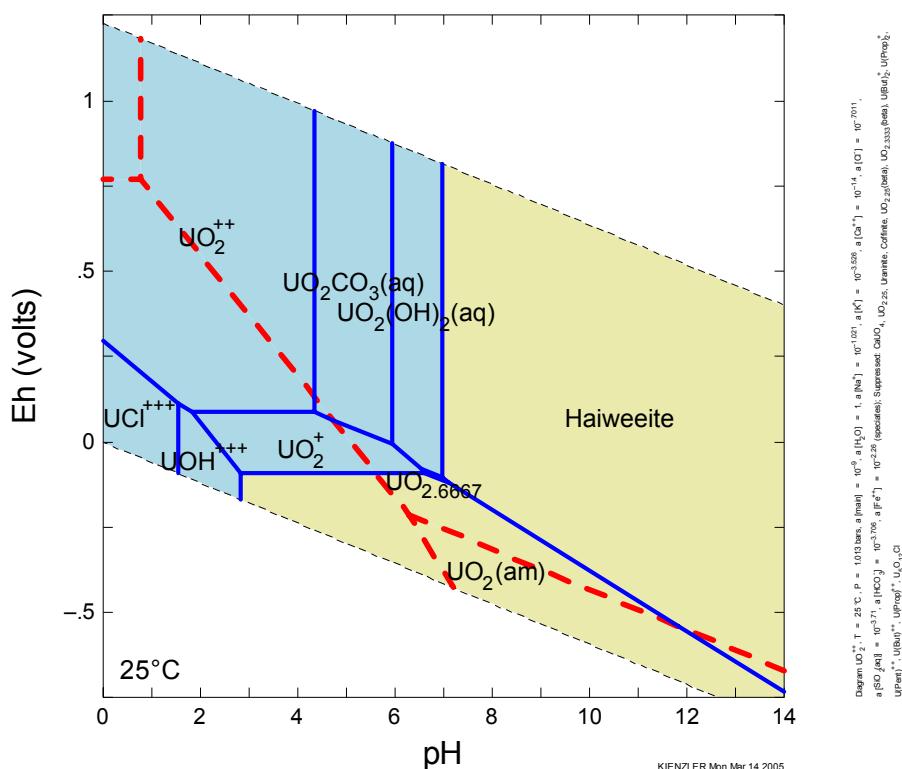


Fig. 18 shows that for pH = 7.3 the transition between U(IV) to U(VI) occurs at a slightly higher redox potential than the Fe(II) to Fe(III) transition. Therefore, O₂-uptake by U oxidation is also expected.

5.4.2 Absolute concentration of U

The speciation of uranium under the conditions of KJ0044F01 groundwater depends on the redox potential (Fig. 19). In the case of E_h = +250 mV, solubility of U(VI) is controlled by U-silicates such as soddyite ((UO₂)₂SiO₄·2H₂O) or haiweeite (Ca(UO₂)₂(Si₂O₅)₃·5H₂O). Resulting solution concentration is computed in the range of 10⁻⁷ to 10⁻⁶ mol l⁻¹. This result bases on the CO₂(g) fugacity of 0.01 bar. As a consequence, uranium carbonate phases are the dominating dissolved species in the relevant pH range. Using the measured HCO₃⁻ concentration of the Chemlab-2 drill hole KJ0044F01 (2002), for 6 ≤ pH ≤ 9, the dominating dissolved uranium species is UO₂(OH)₂. In the case that formation of haiweeite is suppressed or retarded, the soddyite is stable over the relevant pH range.

For reducing conditions, e.g. E_h = -100 mV for pH below 8, U solubility is controlled by UO₂(am): The resulting concentrations are in the range of 10⁻⁹ mol l⁻¹. This value agrees well with the measured U concentrations in native groundwaters KJ0044F01 or SA 2600. This information supports the assumption that observed U in the eluted samples is in the hexavalent state.

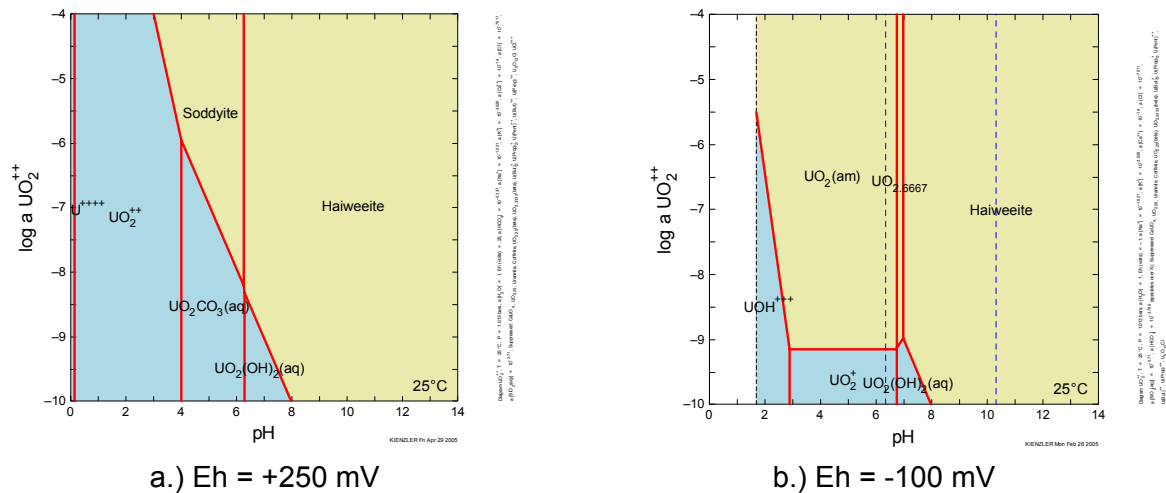


Fig. 19 Speciation of uranium (activity) in the groundwater KJ0044F01 assuming different redox states.

Under the original conditions of granite materials in the Baltic shield (Palmottu, Finland), U is present in the tetravalent redox state forming minerals such as coffinite (USiO₄) (Pomiès et al., 2004). Due to the radioactive decay, uranium concentration in the minerals decreases, leading to a surplus of oxygen which forms U(VI) (Krauskopf, 1982). The U(IV)/U(VI) ratios found in Finish granites are analyzed (Marcos, 2002). The drill cores used for this series of migration experiments were stored for several years in air; oxygen has come into contact to

all open surfaces of the cores. As a consequence, uranium present on the surfaces of the granite (average $6.1 \mu\text{g g}^{-1}$) is oxidized to U(VI) to some extent which is eluted accordingly. To prove this assumption, the U elution of different experiments is compared (Fig. 20).

^{238}U elution from laboratory experiment with core #4 was performed in a glovebox with 99 % Ar /1 % CO_2 atmosphere. ^{238}U was found at the same level ($\sim 10^{-6} \text{ mol l}^{-1}$) as the concentrations determined for the core #7 in-situ experiment. In core #4 experiment, only SA 2600 water was applied having dissolved $[\text{U}] = 2.3 \times 10^{-9} \text{ mol l}^{-1}$ which is in agreement with the solubility of $\text{UO}_2(\text{am})$. In the core #2 in-situ experiment, natural ^{238}U is significantly lower. However, the uranium content of the material used for core #2 amounted only to $3 \mu\text{g g}^{-1}$.

From these findings, it is concluded that the oxidation of U(IV) to U(VI) has already happened in the core under investigation. Consequently, it can be assumed that the availability of oxygen corresponding to measured E_h of 248 mV (SHE) in the groundwater has no additional influence on the uranium mobilization. The reducing capacity of the groundwater is not sufficient to reduce U(VI).

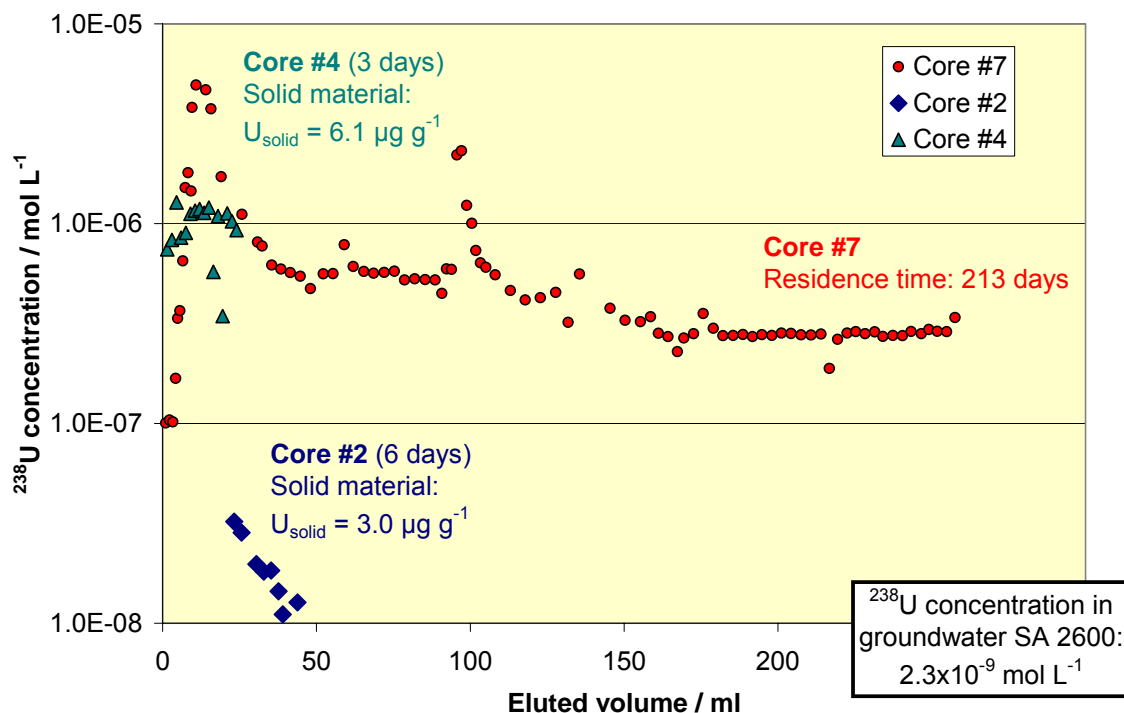


Fig. 20 Elution of natural uranium in three migration experiments.

6 Conclusions from migration and retention experiments

The cores #1 to #5 described in previous reports as well as core #7 are treated in the same way from drilling to application in the migration experiments. Therefore comparisons between the retention behaviour of the different radionuclides as well as some conclusions can be drawn.

Americium

Am(III) exists as mono-carbonato species under the prevailing conditions of laboratory and KJ0044F01 groundwater of the Chemlab-2 site. Both batch experiments with fine grained fracture filling material and with slices of altered material revealed high retention. In the migration experiments, no breakthrough of Am could be detected. By analyzing the cores used in migration experiments in laboratory and in Chemlab-2, retardation coefficients against groundwater of 43 are obtained for a single fracture.

Assuming a groundwater flow rate of $10^{-10} \text{ m s}^{-1}$ which is defined as a minimum criteria for a German repository (AkEnd, 2002), the migration of ^{241}Am remains after 10 half-lives within a distance of ~30 cm. Even in the case that Am is sorbed to stable groundwater colloid, this radionuclide remains in a distance of ~14 m.

Neptunium

Np(V) was used in the experiments. A breakthrough of Np was found in all tests. In laboratory experiments as well as in the in-situ experiment, an initial breakthrough of Np was observed which was unretarded compared to the inert HTO tracer. Recovery of Np varies between zero and 40 % of injected tracer. Speciation of Np by absorption spectroscopy showed only one absorption band of free NpO_2^+ . By comparing the spectroscopic NpO_2^+ concentration to the total Np measured by liquid scintillation counting, the absence of colloids and carbonate complexes was shown. The breakthrough of Np covers an initial pulse due to the reaction kinetics of the retention reaction.

Np(V) is stable in solutions under reducing conditions ($\text{pH} = 7.3$, $\text{Eh} < 0 \text{ mV}$) for long periods of time (more than 0.5 years). In the presence of solid material, however, the reduction process is accelerated significantly. By two independent detection techniques, such as TTA extraction and XPS measurements, the reduction of the initially pentavalent Np to the tetravalent state was proved.

The migration of ^{237}Np is controlled by reduction of Np(V) to Np(IV). If one assumes that 50% of Np is retained within a migration length (length of the cores) of 0.15 m, a Np(V) plume concentration is reduced to 0.1% after a migration distance of 1.5 m independent on the flow rate. In the case of sorbed/reduced Np onto stable groundwater colloids, this radionuclide migrates corresponding to the colloid transport velocity.

Plutonium

Plutonium was used in the tetravalent redox state. Pu sorption takes place on a multitude of minerals. Enhanced sorption onto specific minerals was not observed. However, the retention coefficient is significantly higher compared to Np or U in agreement with migration experiments.

In all migration experiments, Pu concentrations in the eluted water are below the detection limit. Plutonium concentration was retained in the cores close to the location of injection. From core #4 experiments, a lower limit for the retardation factors for Pu in the fracture of $R_s = 135$ was estimated.

Applying the same argumentation and groundwater velocities as in the case of Am, the migration of ^{239}Pu reaches after 10 half-lives a distance of ~ 5.30 m from the source. However, plutonium has the tendency to be sorbed onto all kind of groundwater colloids, which migrates corresponding to the colloid transport velocity.

Uranium

For all experiments U(VI) was used. At the pH of the groundwater, $\text{UO}_2(\text{OH})_2(\text{aq})$ is expected to dominate speciation. From batch experiments it was shown that U(VI) retention is correlated to Fe-bearing mineral phases. The retention rate is clearly slower and the absolute retention coefficient is by an order of magnitude lower than in the case of other actinides such as Am or Pu. Determination of the retention properties in the fractured core reveals a retardation coefficient with respect to an inert tracer of $R_s = 3.9 - 5$. The recovery of the U tracer was above 30%. Indications for matrix diffusion processes for natural ^{238}U were detected.

This finding correlates with the observed migration behaviour of natural U. It was shown clearly that natural uranium is mobilized from the rock sample. The mobilization and elution behaviour requires a pre-oxidization of U-minerals which is expected and described in literature. Eluted concentrations of natural U are in the range of 20 - 200 ppm, concentrations significantly above the concentrations of undisturbed granite groundwaters. For an experimental period of 10 month, no decrease of the U concentration was observed.

The behaviour of natural uranium requires consideration in performance assessment of a repository. The interaction of the disturbed host rock with air may cause an oxidation of U minerals. By this process, the background U concentration in nearby groundwaters may increase significantly.

Technetium

For the batch and migration experiments Tc(VII) was used. In batch experiments, Tc shows pronounced sorption kinetics. Tc retention is not necessarily correlated to high Fe concentrations in the mineral phases. XPS analyses show a clear shift of Tc binding energy to a reduced redox state. This is explained by the fact that Tc undergoes reduction in the solution. A solid surface - as in the case of Np - is not a requirement for the reduction of Tc(VII) to Tc(IV).

The migration experiments show an initial breakthrough of ^{99}Tc . After this peak, Tc concentration decreases to values close to the detection limit.

7 Outlook

The in-situ migration experiment with core #7 will terminate the series of Actinide Migration Experiments. Before recovery of the core, a special test is planned. This test should give additional information of the effect of matrix diffusion. The following test procedure is planned. Chemlab 2 flow is stopped completely for two weeks in order to allow out diffusion of U from the rock matrix of core #7 into the fracture. After this interruption period, Chemlab will be restarted at the same flow rate as before and sampling will be continued for several weeks. Afterwards, the experiment will be terminated and the core, reservoir and samples send to FZK for detailed investigations. Core #7 will be fixed in epoxy, cut and analyzed with respect to retained radionuclides.

To obtain insight in the behaviour of colloids under conditions relevant to the situation in the vicinity of a repository in deep underground, a dipole experiment is planned on the transport of colloids and colloid facilitated transport of radionuclides. For preparation of such experiments, the existence and properties of natural aquatic colloids present in the selected groundwater are of particular importance. At Äspö HRL, suited drillholes will be selected for these investigations. Within a stay of a Swedish post-doc scientist at INE, a study on stability and preparation of colloids will be performed as well as the characterisation of size and properties of the colloids to be injected. As an outcome of these laboratory investigations, the design of the colloid migration study will be defined. The stability of a colloid bearing cocktail will be investigated and prepared to be used in CHEMLAB 2. Core #6 will be inserted and an actinide-colloid experiment can be performed in CHEMLAB 2 using the sampling and analysis procedure as in the previous experiments. This experiment will provide information for designing a dipole experiment.

Acknowledgment

The work was performed within the Project Agreement for collaboration on certain experiments related to the disposal of radioactive waste in the Hard Rock Laboratory Äspö (HRL) between the German Bundesministerium für Wirtschaft und Arbeit (BMWA) and Svensk Kärnbränslehantering AB (SKB).

The authors thank the staff of Äspö HRL for preparation of rock and water samples, for the excellent cooperation and the maintenance of our glovebox.

8 References

- Aamrani, F.E. et al., 1999. Experimental and modeling study of the interaction between uranium (VI) and magnetite. TR-99-21, Svensk Kärnbränslehantering AB, Stockholm, Sweden.
- AkEnd, 2002. Site Selection Procedure for Repository Sites: Recommendations of the AkEnd, AkEnd - Committee on a Site Selection Procedure for Repository Sites.
- Appelo, C.A.J. and Postma, D., 1993. Geochemistry, groundwater and pollution. A.A. Balkema, Rotterdam.
- Bäckblom, G., 1991. The Äspö hard rock laboratory - a step towards the Swedish final repository for high-level radioactive waste. *Tunnelling and Underground Space Technology*, 4: 463-467.
- Baik, M.H., Hyun, S.P., Cho, W.J. and Hahn, P.S., 2004. Contribution of minerals to the sorption of U(VI) on granite. *Radiochimica Acta*, 92: 663-669.
- Crank, J., 1978. The mathematics of diffusion. Clarendon Press, Oxford, UK.
- Ilton, E.S. et al., 2004. Heterogeneous reduction of uranyl by micas: Crystal chemical and solution controls. *Geochim. Cosmochim. Acta*, 68(11): 2417-2435.
- Jansson, M. and Eriksen, T.E., 1998. CHEMLAB In-Situ Diffusion Experiments Using Radioactive Tracers. *Radiochimica Acta*, 82: 153-166.
- Kienzler, B., Römer, J., Schild, D. and Bernotat, W., 2003a. Sorption of actinides onto granite and altered material from Äspö HRL. In: V.M. Oversby (Editor), Scientific Basis for Nuclear Waste Management XXVII., Kalmar, June 16-18, 2003., MRS Symp.Proc. 807, 2004: 665-70
- Kienzler, B. et al., 2002. Actinide migration in granite fractures: comparison between in-situ and laboratory results, Scientific Basis for Nuclear Waste Management XXVI, Symp.II, MRS Fall Meeting, Boston, Mass., December 2-6, 2002. MRS Symp.Proc. 757, 2003: II11.2/1-6
- Kienzler, B. et al., 2003b. Swedish-German actinide migration experiment at ÄSPÖ HRL. *Journal of Contaminant Hydrology*, 61: 219-233.
- Kienzler, B. et al., 2003c. Actinide migration experiment in the ÄSPÖ HRL in Sweden: results from Core #5 (Part III). FZKA 6925, Forschungszentrum Karlsruhe.
- Krauskopf, K.B., 1982. Introduction to Geochemistry. McGraw-Hill Book Co.
- Kunze, S., Neck, V., Gompper, K. and Fanghaenel, T., 1996. Studies on the immobilization of technetium under near field geochemical conditions. *Radiochimica Acta*, 74: 159163.
- Marcos, N., 2002. Lessons from nature – The behaviour of technical and natural barriers in the geological disposal of spent nuclear fuel, Helsinki University of Technology (HUT), Espoo, Finland.
- Pomiès, C., B.Hamelin, J.Lancelot and R.Blomqvist, 2004. $^{207}\text{Pb}/^{206}\text{Pb}$ and $^{238}\text{U}/^{230}\text{Th}$ dating of uranium migration in carbonate fractures from the Palmottu uranium ore (southern Finland). *Applied Geochemistry*, 19(3): 273-288.
- Puigdomenech, I. et al., 2001. O₂ depletion in granitic media: The REX project. TR 01-05, Swedish Nuclear Fuel and Waste Management Co (SKB), Stockholm Sweden.
- Rodrigues, E. et al., 1998. Surface characterization of olivine-rock by X-ray photoelectron spectroscopy (XPS). Leaching and U(VI)-sorption experiments. *Mat. Res. Soc. Symp. Proc.* 506: 321-327.
- Römer, J. et al., 2002. Actinide migration experiment in the HRL ÄSPÖ, Sweden: results of laboratory and in situ experiments (Part II). FZKA 6770, Forschungszentrum Karlsruhe.
- Vejmelka, P. et al., 2000. Sorption and Migration of Radionuclides in Granite (HRL ÄSPÖ, Sweden). FZKA 6488.
- Vejmelka, P. et al., 2001. Actinide migration experiment in the HRL ÄSPÖ, Sweden: Results of laboratory and in-situ experiments (Part I). FZKA 6652, Forschungszentrum Karlsruhe.
- Widestrand, H., Byegård, J., Ohlsson, Y. and Tullborg, E.-L., 2003. Strategy for the use of laboratory methods in the site investigations programme for the transport properties of the rock. R 03-20, Swedish Nuclear Fuel and Waste Management Co (SKB), Stockholm Sweden.

Appendix A Tables

Surface	Analysis Area	O	C	Si	Al	Mg	Ca	Na	K	Fe	Ti	P	N	S	Cl	F	Cu	Tc
Polished	# 1	47.71	27.18	11.08	6.54	0.86	1.99	0.70	---	1.26	0.42	0.27	1.43	0.20	0.18	0.19	---	---
Polished	#2	48.45	28.49	10.69	5.38	0.80	1.91	0.24	---	1.01	0.25	---	1.66	0.55	0.22	0.22	---	0.11
Polished	#3	48.72	23.78	11.24	6.30	1.20	1.80	1.03	0.11	1.96	0.29	---	1.79	0.88	0.12	0.58	---	0.17
As cut	#4	40.70	37.12	5.91	4.62	2.60	1.09	---	---	2.17	0.34	---	4.13	0.80	0.09	0.30	---	0.12
As cut	#5	51.02	21.12	15.86	5.72	---	0.48	2.48	0.72	---	---	---	2.14	0.23	0.15	0.04	---	0.04
As cut	#6	42.96	33.73	8.24	5.79	0.60	0.55	1.13	0.35	0.73	---	---	4.29	1.26	---	---	0.21	0.16

XPS investigations of Tc sorption: Atomic concentrations calculated by the elemental lines of XPS survey spectra at different areas of the sample (diameter 0.8 mm each). Relative error (10-20) %. Cu results from the cutting blade.